J|A|C|S
ARTICLES
Published on Web 10/27/2006

Electrochemical Origin of Voltage-Controlled Molecular Conductance Switching

Jin He,[†] Qiang Fu,[†,‡] Stuart Lindsay,*[,†,‡,§] Jacob W. Ciszek,[||] and James M. Tour[||]

Contribution from the Biodesign Institute, Department of Chemistry, and Biochemistry and Department of Physics and Astronomy, Arizona State University, Tempe, Arizona 85287, and Department of Chemistry and the Smalley Institute for Nanoscale Science and Technology, Rice University, Houston, Texas 77005

Received May 21, 2006; E-mail: Stuart.Lindsay@asu.edu

Abstract: We have studied electron transport in bipyridyl-dinitro oligophenylene-ethynelene dithiol (BPDN) molecules both in an inert environment and in aqueous electrolyte under potential control, using scanning tunneling microscopy. Current−voltage (*IV*) data obtained in an inert environment were similar to previously reported results showing conductance switching near 1.6 V. Similar measurements taken in electrolyte under potential control showed a linear dependence of the bias for switching on the electrochemical potential. Extrapolation of the potentials to zero switching bias coincided with the potentials of redox processes on these molecules. Thus switching is caused by a change in the oxidation state of the molecules.

Introduction:

Molecular electronics[1−4] has attracted a tremendous amount of interest in the past decade. Molecular memories and switches require a nonlinear response, and molecules with well-defined and readily accessible redox states are attractive candidates. Redox-active molecules have been shown to exhibit properties such as negative differential resistance (NDR),[5−8] switching,[9−12] and rectification.[13] In this paper, we are concerned with the nonlinear conductance behavior of conjugated phenylene-ethyneylene oligomers with electroactive nitro functional groups. These molecules were previously studied in nonelectrolytes where potential control is not possible.[12,14−17] The origin of the reported nonlinear current−voltage (*IV*) characteristic is still not well understood. In particular, it is difficult to correlate events in the *IV* characteristics with the redox properties of the molecules in two-electrode experiments where the potential at the molecule is not well determined.[18]

Blum et al.[9] demonstrated that the bipyridyl-dinitro oligophenylene-ethynelene dithiol (BPDN) molecule can switch between two conductance states in air using several different measurement techniques. Switching was also observed by Khondaker et al.,[19] who found it did not require the nitro group. Here we report a study of BPDN molecular conductance-switching behavior by STM both in an inert environment and under potential control in an electrolyte solution.

In this study we find two types of behavior: (a) A rapid jump in the conductance when a particular bias is reached, the conductance remaining at its new value for the rest of the bias sweep. We call this a "switching event". (b) A continuous (and often reversible) change of conductance in which the current passes through a peak value and then falls back to a smaller value. We call this a "current peak" or "NDR peak" (NDR for negative differential resistance). Both types of behaviors are often seen in one curve. We found a strong correlation between the value of bias that causes switching and current peaks and the electrochemical potential of BPDN molecules, leading us to the conclusion that the bias-induced switching of the BPDN molecule is a consequence of the change of oxidation state of the molecule.

[†] Biodesign Institute, Arizona State University.
[‡] Department of Chemistry, Arizona State University.
[§] Department of Physics and Astronomy, Arizona State University.
[||] Rice University.

(1) Mirkin, C. A.; Ratner, M. A. *Annu. Rev. Phys. Chem.* **1992**, *43*, 7389−7396.
(2) Nitzan, A.; Ratner, M. A. *Science* **2003**, *300*, 1384−1389.
(3) Joachim, C.; Gimzewski, J. K.; Aviram, A. *Nature* **2000**, *408*, 541−548.
(4) McCreery, R. L. *Chem. Mater.* **2004**, *16*, 4477−4496.
(5) Chen, J.; Reed, M. A.; Rawlett, M. A.; Tour, J. M. *Science* **1999**, *286*, 1550−1552.
(6) Chen, F.; He, J.; Nuckolls, C.; Roberts, T.; Klare, J. E.; Lindsay, S. M. *Nano Lett.* **2005**, *5*, 503−506.
(7) Xiao, X.; Nagahara, L. A.; Rawlett, A. M.; Tao, N. *J. Am. Chem. Soc.* **2005**, *127*, 9235−9240.
(8) Wassel, R., A.; Credo Grace, M.; Fuierer Ryan, R.; Feldheim Daniel, L.; Gorman Christopher, B. *J. Am. Chem. Soc.* **2004**, *126*, 295−300.
(9) Blum, A. S.; Kushmerick, J. G.; Long, D. P.; Patterson, C. H.; Yang, J. C.; Henderson, J. C.; Yao, Y.; Tour, J. M.; Shashidhar, R.; Ratna, B. R. *Nat. Mater.* **2005**, *4*, 167−172.
(10) Cai, L.; Cabassi, M. A.; Yoon, H.; Cabarcos, O. M.; McGuiness, C. L.; Flatt, A. K.; Allara, D. L.; Tour, J. M.; Mayer, T. S. *Nano Lett.* **2005**, *5*, 2365−2372.
(11) Gergel, N.; Majumdar, N.; Keyvanfar, K.; Swami, N.; Harriott, L. R.; Bean, J. C.; Pattanaik, G.; Zangari, G.; Yao, Y.; Tour, J. M. *J. Vac. Sci. Technol. A* **2005**, *23*, 880−885.
(12) Li, C.; Zhang, D.; Liu, X.; Han, S.; Tang, T.; Zhou, C.; Fan, W.; Koehne, J.; Han, J.; Meyyappan, M.; Rawlett, A. M.; Price, D. W.; Tour, J. M. *Appl. Phys. Lett.* **2003**, *82*, 645−647.
(13) Metzger, R. M. *Chem. Rev.* **2003**, *103*, 3803−3834.
(14) Fan, F.-R. F.; Yang, J.; Dirk, S. M.; Price, D. W.; Kosynkin, D.; Tour, J. M.; Bard, A. J. *J. Am. Chem. Soc.* **2001**, *123*, 2454−2455.
(15) Fan, F.-R. F.; Yao, Y.; Cai, L.; Cheng, L.; Tour, J. M.; Bard, A. J. *J. Am. Chem. Soc.* **2004**, *126*, 4035−4042.
(16) Fan, F.-R. F.; Lai, R. Y.; Cornil, J.; Karzazi, Y.; Bredas, J.-L.; Cai, L.; Cheng, L.; Yao, Y.; Price, D. W.; Dirk, S. M.; Tour, J. M.; Bard, A. J. *J. Am. Chem. Soc.* **2004**, *126*, 2568−2573.
(17) Kratochvilova, I.; Kocirik, M.; Zambova, A.; Mbindyo, J.; Malloukc, T. E.; Mayer, T. S. *J. Mater. Chem.* **2002**, *12*, 2927−2930.
(18) He, J.; Lindsay, S. M. *J. Am. Chem. Soc.* **2005**, *127*, 11932−11933.
(19) Khondaker, S. I.; Yao, Z.; Cheng, L.; Henderson, J. C.; Yao, Y.; Tour, J. M. *Appl. Phys. Lett.* **2004**, *85*, 645−647.

10.1021/ja0635433 CCC: $33.50

For measurements made under potential control, we have acquired data two ways. In the first type of measurement we measure current as a function of tip-to-substrate bias at constant surface potential (though one result of this work is we find that tip bias can alter the local electrochemical potential). We call these "*IV* measurements". In the second type of measurement, we record current as a function of the electrochemical surface potential at constant tip−substrate bias. We call these "*IE* measurements". *IE* measurements were first demonstrated by Tao,[20] who studied iron porphyrin on a highly oriented pyrolytic graphite (HOPG) surface and found a significant tunneling current enhancement near the iron center's redox potential. Several groups have since demonstrated similar behavior in various redox molecules.[6,21−23] It is common to refer to the "electrode potential" when measurements are made under electrochemical potential control. We have two electrodes in this experiment: the surface (which is under direct potential control) and the tip (which is biased with respect to the surface). So we will use "surface potential" to refer to the imaging surface and "tip potential" to refer to the probe.

Both *IE* and *IV* measurements showed both switching and (usually) a reversible current peak as a function of potential. The bias at which these events were observed in *IV* measurements depended on both tip−substrate bias and the electrochemical potential in a way that reflected the change of local potential induced by the tip−substrate bias. Similar types of events (at similar bias) were observed in *IV* measurements made *without* potential control, suggesting that the switching observed in ambient conditions also arises from redox processes. However, data obtained in air were less reversible with fewer current peaks and relatively more switching events, showing that the presence of a supporting electrolyte changes the mechanism somewhat.

Methods

Synthesis. The three molecules (**1a**, **1b**, and **2**) used in our experiments are shown below. The synthesis of compound **1a** has been reported previously.[24] Transformation of **1a** to **1b** occurs via an acid-

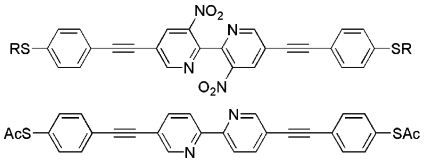

1a BPDN R=Ac

1b BPDN R=H

2 BP

catalyzed deprotection whereupon **1b** was isolated and characterized. BP was synthesized via Sonagashira coupling of 5,5′-diiodopyridine with 4-ethynyl(thioacetyl)benzene. Details of the molecular synthesis (including characterization data) can be found in the Supporting Information.

SAM Preparation and Calibration. 1b was dissolved to a final concentration of ca. 1−10 mM in Ar-purged DMF or DMSO and deposited onto a freshly hydrogen-flame-annealed Au(111) substrate[25] for 12 h at room temperature in the dark in a nitrogen-purged glovebox (O_2 level < 2 ppm). A longer deposition time (∼48 h) was needed for **1a**. During assembly no acid or base was added (i.e., for deprotection of **1a**) to avoid any possible side reactions.[7,26] The data we recorded for **1a** and **1b** showed no noticeable difference, and thus we will not differentiate between them, referring to both types of sample as BPDN in what follows. The thickness of the BPDN self-assembled monolayer (SAM) after deposition was monitored by ellipsometry (Gaertner, Skokie, IL) at a wavelength of 632.8 nm with an incident angle of 70°. The optical constants of the bare gold substrate were measured before deposition of molecules giving $n \approx 0.18$ and $k \approx -3.53$, values slightly different from bulk gold. The BPDN SAM optical constants were set to $n_f = 1.55$ and $k_f = 0$ using literature values.[27] The length of BPDN and BP calculated using AM1molecular mechanics were 2.394 and 2.399 nm, respectively (from sulfur to sulfur). The measured thickness of the SAM of BPDN is between 1.8 and 2 nm. The SAM of BP was prepared the same way as that for BPDN, and the thickness was found to around 2.2∼2.5 nm.

STM Setup and *IV* Measurements without Potential Control. STM measurements were performed with a PicoSTM system (Molecular Imaging, Tempe). The STM tip was formed by cutting a 0.25 mm-diameter Au wire (Alfa Aesar, 99.999%). The gold tips were immersed in Piranha Solution (3:1 H_2SO_4/H_2O_2, 30 vol %; *use caution as this solution is extremely caustic and will explode on contact with organics*) for 30 s, rinsed with DI water, and dried in an Ar stream prior to use or wax coating. Insulated probes were formed by coating the gold tip with Apiezon wax.[28] Ag and Pt wires were used for the reference and counter electrodes, respectively. They were sonicated for 10 min in acetone, methanol, and DI water in turn and dried in an N_2 stream. The Pt wire was further cleaned in a hydrogen flame before use. The SAM was rinsed copiously with DMF or DMSO, dried in an argon stream, and then placed in the liquid cell of the STM under argon-purged toluene or an aqueous solution (containing 50mM $Na_2B_4O_7$), and maintained under argon in an environmental chamber.

The surface was first imaged in constant current mode to ensure that a clean submonolayer was present. Then the argon flow and feedback loop were turned off, and the tip−substrate distance was adjusted manually (using Labview software) until a stable current was maintained, indicating that a molecule was stably trapped between the probe and substrate. Normally several hours were required for the microscope to stabilize mechanically. Once stable, these measurements would yield tunneling currents that stayed at the set-point value (without feedback control) for up to 10 s, indicating that the drift in the gap was very small. *IV* curves were acquired starting from initial currents of less than 30 pA (the leakage current is normally 2−5 pA at the highest bias) with a tip−sample bias of 100 mV. After this initial condition was established, *IV* curves were recorded by sweeping the bias from the set-point value and acquiring the corresponding current data with a digital oscilloscope interfaced to a National Instruments data acquisition card (using a breakout box to interface with the PicoSTM).

***IE* and *IV* Measurement under Potential Control.** The STM setup for *IE* and *IV* measurements under potential control is illustrated in Figure 1a. Bias V ($= -V_{ts}$) is the tip-to-substrate potential difference (with the sign convention such that positive bias denotes electron tunneling from the tip to the substrate). This complication arises because the substrate is biased with respect to the ground of the electrochemical system (see Figure 1a). E_s and E_t are the surface potential and tip potential with respect to the reference electrode. They are adjusted by the microscope's internal potentiostat such that

$$E_t = E_s - V \quad (1)$$

It is important to note that we record two types of current during these experiments. The total electrochemical current is the current

(20) Tao, N. *Phys. Rev. Lett.* **1996**, *76*, 4066−4069.
(21) Gittins, D. I.; Bethell, D.; Schriffrin, D. J.; Nichols, R. J. *Nature* **2000,** *408*, 67−69.
(22) Albrecht, T.; Guckian, A.; Ulstrup, J.; Vos, J. G. *Nano Lett.* **2005**, *5*, 1451−1455.
(23) Xu, B. Q.; Xiao, X. Y.; Yang, X.; Zang, L.; Tao, N. J. *J. Am. Chem. Soc.* **2005**, *127*, 2386-2387.
(24) Flatt, A. K.; Tour, J. M. *Tetrahedron Lett.* **2003**, *44*, 6699−6702.
(25) DeRose, J. A.; Thundat, T.; Nagahara, L. A.; Lindsay, S. M. *Surf. Sci.* **1991**, *256*, 102−108.
(26) Stapleton, J. J.; Harder, P.; Daniel, T. A.; Reinard, M. D.; Yao, Y.; Price, D. W.; Tour, J. M.; Allara, D. L. *Langmuir* **2003**, *19*, 8245−8255.
(27) Cai, L.; Yao, Y.; Yang, J.; Price, D. W.; Tour, J. M. *Chem. Mater.* **2002**, *14*, 2905−2909.
(28) Nagahara, L. A.; Thundat, T.; Lindsay, S. M. *Rev. Sci. Instrum.* **1989**, *60*, 3128−3130.

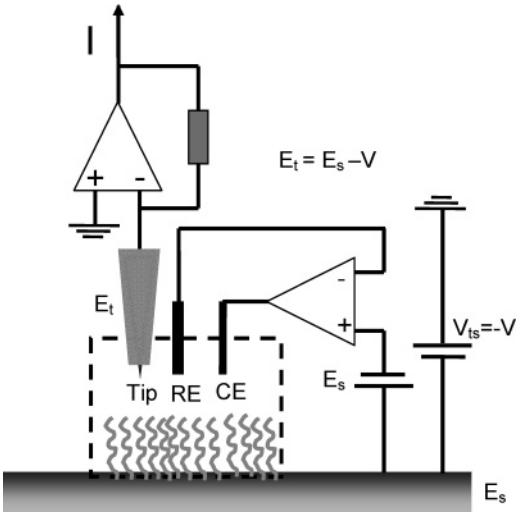

Figure 1. Schematic of the STM setup for measurements under potential control. E_t is the tip potential, E_s is the surface potential, and V is the substrate bias with respect to ground. In practice, the potentiostat sets E_s relative to the substrate by compensating for the applied bias, V. RE and CE are the reference and counter electrode, respectively, and are placed macroscopic distances from the substrate (scheme is not to scale). The tip is coated with insulation to minimize Faradaic current.

measured between the counter electrode (CE in Figure 1) and working electrode (the gold substrate). This is the current recorded for conventional cyclic voltammograms. We also measure a tip-to-substrate (local) current which we will refer to as the "tunneling current". It can contain a small electrochemical component (Faradaic current), but the tips are insulated to minimize this so that it is a small fraction of the measured tunnel current.

Similar experiments[6] have shown that the local potential is modified strongly by the applied bias when a molecule is chemically bonded across the two electrodes. Following the approach previously reported,[6] we calculate the local potential under the tip through a simple model that assumes that the interfacial field and the field generated by the tip are additive, giving rise to an effective local potential, E, given by

$$E = E_s - \alpha V \quad (2)$$

where α is a constant that depends on geometry. If the potential owing to the tip is half the applied bias (expected for a symmetrical junction), then $\alpha = 0.5$. $\alpha > 0.5$ implies that the applied bias alters the local potential under the tip *more* than the interfacial polarization. This is possible because, in addition to generating a local field, the tip may also screen the local polarization, thus lessening the effect of macroscopic alterations in surface potential in the region immediately under the tip. We have observed $\alpha > 1$ in previous work.[6,29] On the other hand, complete screening of the applied bias by the double layer corresponds to $\alpha = 0$. This is the case when the tip is far from the surface (i.e., much more than a Debye length, roughly 1 nm here).

During *IE* measurement, E_t and E_s were varied together so as to keep the potential difference (V) between tip and substrate fixed, and both tunneling (i.e., tip to substrate) current and the total electrochemical current were recorded as a function of E_s.

For *IV* measurements, E_s was fixed while the magnitude of E_t was increased linearly with time (with a corresponding increase in V_{ts}) while we recorded the current through the probe (i.e., the "tunneling current"). Tips were tested for Faradaic leakage again after each experiment to ensure that the insulation had remained intact. In addition to the potential-dependent events we report here, potential-independent switching events were occasionally observed, and we attribute these to the molecule-metal bond fluctuations reported by Ramachandran et al.[30]

The electrochemical properties of the BPDN SAM were verified by cyclic voltammetry carried out with the microscope's built-in potentiostat. Cyclic voltammograms were collected simultaneously with *IE* measurements as the surface potential was swept for the *IE* recording. In the case of *IV* measurements (which were taken at constant E_s), cyclic voltammograms were recorded between *IV* sweeps. The shape of the cyclic voltammogram was quite stable at low oxygen levels. Increases in the Faradaic current beyond $E_s = -0.66$ V indicated increased oxygen concentration. When this occurred, we stopped the data collection and restored the argon flow to the environmental chamber until stable voltammetry was restored.

Results

We begin with the cyclic voltammetry (CV) of BPDN and BP in the aqueous electrolyte used for the electronic measurements. CV data were better resolved in nonaqueous electrolyte, and these data are presented in the Supporting Information as confirmation of the results obtained in aqueous electrolyte. We then present the results of *IV* measurements obtained in toluene, showing how they duplicate previously reported switching events. We turn next to *IV* measurements under potential control, demonstrating the interplay between applied bias and electrochemical potential. These results are confirmed by complementary *IE* measurements made at different (fixed) values of tip-to-substrate bias.

(a) Cyclic Voltammetry. Cyclic voltammograms (CV) were collected both in DMF electrolyte (0.1 M $TBABF_4$) and in aqueous electrolyte (50 mM sodium tetraborate). CVs were collected in situ on the microscope using a silver wire quasi reference electrode. We calibrated the potential relative to the SCE standard reference electrode using both potassium ferricyanide and the reduction potential of a previously oxidized gold surface. Our quasi-reference was found to be shifted 140 mV positive of the SCE and stable to within 50 mV from run to run. Potentials in this paper will henceforth be quoted vs the SCE.

Several typical cycles of in situ CVs of BPDN in 50mM $Na_2B_4O_7$ aqueous solution are shown in Figure 2a. The first redox process at ca. -0.47V vs SCE (labeled R1/O1) was sometimes hard to observe, was not reversible, and disappeared on repeated cycling in aqueous electrolyte. The second process at ca. -0.67 V (labeled R2/O2) was more readily observed and more reversible. (Both redox peaks are more clearly resolved in organic solvent and a typical CV is shown in the Supporting Information.) The first cycle of the CV was somewhat different from subsequent cycles indicative of some changes in the adsorbate. R2/O2 were quite stable in the second and subsequent CV sweeps as long as the oxygen level was low and the potential was kept above -0.76 V (where reduction of the thiol occurs;[31] see Supporting Information). Based on the reduction peak R2 of Figure 2a and assuming a one-electron process, the surface concentration of BPDN molecules was calculated to be about 6.7×10^{-11} mol/cm^2, which is 17% to 58% of a full monolayer (depending on the possible range of molecular adsorption geometries and assuming a gold surface roughness factor of

(29) Chen, F.; Nuckolls, C.; Lindsay, S. M. *Chem. Phys.* **2006**, *324*, 236−243.

(30) Ramachandran, G. K.; Hopson, T. J.; Rawlett, A. M.; Nagahara, L. A.; Primak, A.; Lindsay, S. M. *Science* **2003**, *300*, 1413−1415.

(31) Carot, M. L.; Esplandiu, M. J.; Cometto, F. P.; Patrito, E. M.; Macagno, V. A. *J. Electroanal. Chem.* **2005**, *579*, 13−23.

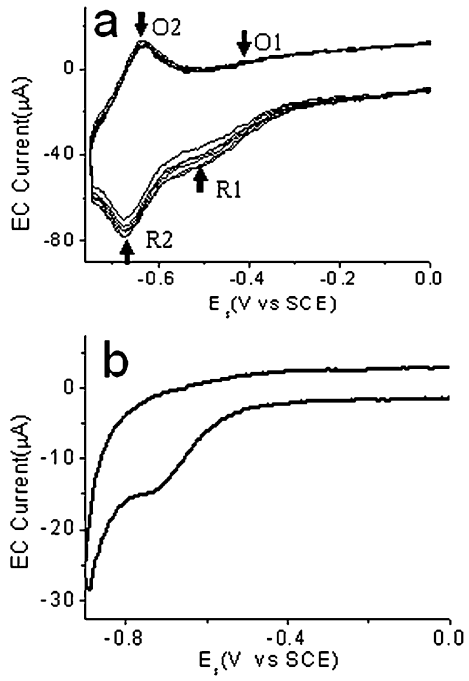

Figure 2. (a) Cyclic voltammograms for BPDN (6 sweeps). A reversible wave is seen at O2 and R2 (−0.67 V vs SCE) and a nonreversible wave (R1/O1) is observed near −0.48 V. O1 is only distinctly resolved in organic solvent (see Supporting Information). The sweep rate is 250 mV/s. (b) Cyclic voltammograms for BP swept at 250 mV/s. A nonreversible reduction wave is observed at about −0.73 V.

1.3). The CV of BP is shown in Figure 2b. A reduction peak near −0.71 V was clear but was not reversible and gradually disappeared on cycling.

The nonreversible reduction peak R1 of BPDN in Figure 2a (which does not appear in the CV of BP) may be due to the NO_2 group in BPDN. Xiao et al. found that the NO_2 group reduction was nonreversible in aqueous solution.[7] The second reversible peak R2 may be due to the contributions of both the NO_2 group and the pyridine groups because BP showed a nonreversible reduction peak at −0.73 V, but BPDN showed a reversible peak at −0.68 V.

(b) *IV* Measurements in Toluene. *IV* measurements were first performed in freshly distilled toluene (sparged with high purity argon that had been passed through an oxygen scavenging system). Our results were similar to those of Blum et al.[9] Significant hysteresis was observed, and the switching bias ($-V_{ts}$) was around 1.6 V over the range of scan rates studied (0.1 V/s to 20 V/s). We also scanned the bias from −0.1 V to 2 V and then back to −0.1 V at 10 V/s repeatedly. The current became noisier after two cycles which we attribute to tip drift (because more cycles could be scanned without noise if the scan rate was higher). One typical curve with two bias cycles is shown in Figure 3a. The black curve shows the first cycle and the gray curve shows the second cycle, and events are numbered in the order in which they occur. The molecule switched to a high conductance in a bias range between 1.4 and 1.9 V after which it stayed in a high conductance state. At the beginning of the second cycle, the molecule remained in a high conductance state, and the current retraced that recorded in the first cycle. The molecule then switched to a low conductance near 1.5 V and retraced the previous cycle again on the return to −0.1 V. As listed in Table 1, current switching near a bias of 1.64 V occurred in 80% of the total sweeps (discounting featureless and noisy *IV* curves). The remaining 20% showed peaks in the current (NDR). These peaks were generally not reversible. An example of such a curve is shown in Figure 3b. A current peak is evident near 1.6 V in the forward bias sweep (black curve) but is not observed in the backward bias sweep (gray curve).

(c). *IV* Measurements under Potential Control. We conducted further *IV* measurements in an aqueous solution of 50 mM $Na_2B_4O_7$ under potential control. The bias was typically swept at 1 V/s for a total sweep time of 2 s. Similar conductance switching events and current peaks were observed but at a much reduced bias. The first two columns of Table 1 contrast results from *IV* measurements without and with potential control (for $E_s = 0.14$ V vs SCE). These are the averages of data obtained from several hundred curves. The switching bias drops from ca. 1.6 V to 0.8 V when the molecules are held at a potential of 0.14 V vs SCE. Similarly the bias for a maximum in NDR peaks shifts from 1.7 to 0.8 V. The fraction of switching events to total events (switching plus peaks) falls from 0.8 for *IV* curves taken without potential control to ca. 0.5 under potential control. Switching events are rarer still (0.2) in *IE* curves (discussed below).

In addition to the switching events, 53% of sweeps showed NDR peaks (Table 1). The position of both switching events and NDR peaks changed with potential in a systematic way as shown in Figure 4 (switching events parts a−c, NDR peaks parts d−f). As the electrochemical potential is reduced, the bias at which a switching event or NDR peak occurs is reduced. Data are less noisy taken under potential control, and histograms of the bias for switching or NDR peaks show evidence of three peaks that were not resolved in the switching bias for data taken without potential control (insets in Figure 4). We have averaged all data within ±0.15 V of each apparent peak, and the mean and standard deviation of each of these distributions for each of the three peaks are reported for three values of potential (−0.06, 0.14, and 0.34V vs SCE) in Table 2. These data are plotted in Figure 5 (part a, switching events; part b, NDR peaks). The bias for switching or NDR peaks clearly falls linearly with potential, in agreement with eq 2. Rearranging this relationship to express the switching potential, V_p, as a function of surface potential at a given bias, $E_s(V)$, yields

$$V_p = \alpha^{-1}(E_s(V) - E_p(0)) \qquad (3)$$

Here $E_p(0)$ is the potential for switching at zero applied bias. Fits of eq 3 to the data shown in Figure 5 (lines) yield the values for α and E_p shown in the last two columns of Table 2. We see that $\alpha \approx 1$ in all cases, similar to what has been observed in several other molecules in electrochemically controlled break junctions.[6,29,32] The major peak in the distribution (peak 3) is fitted with $E_p = -0.69 \pm 0.2$ V (switching) and $E_p = -0.67 \pm 0.08$V vs SCE (NDR peaks). These values are in good agreement with the potential for the second redox process (R2/O2, $E = -0.67$ V vs SCE). The next most significant peak (peak 2) is fitted with $E_p = -0.48 \pm 0.01$ V (switching) and $E_p = -0.49 \pm 0.02$ V vs SCE, in agreement with the potential of the first redox process (R1/O1 at ca. −0.47 V vs SCE). The

(32) Visoly-Fisher, I.; Daie, K.; Terazono, Y.; Herrero, C.; Fungo, F.; Otero, L.; Durantini, E.; Silber, J. J.; Sereno, L.; Gust, D.; Moore, T. A.; Moore, A. L.; Lindsay, S. M. *Proc. Natl. Acad. Sci. U.S.A.* **2006**, *103*, 8686−8690.

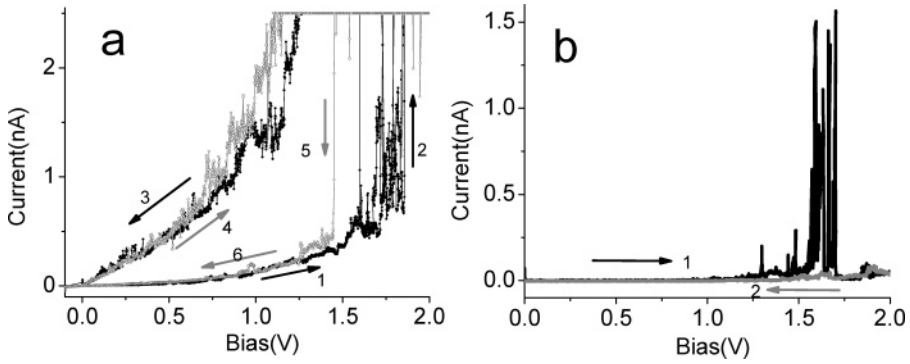

Figure 3. Typical *IV* curves taken in toluene showing (a) switching and (b) NDR peaks. Data were collected at a sweep rate of 10 V/s and a starting current at 10−50 pA/0.1 V. In (a) the black curve was the first cycle and gray curve was the second cycle (arrows indicate the time sequence). The current amplifier saturated at 2.5 nA. In (b) the black curve is a forward sweep, and the gray curve is a backward sweep.

Table 1. Switching Bias and Peak−Peak Bias for *IV* Curves for Molecules in Toluene, under Potential Control and Also for *IE* Curves

experiment methods	IV in toluene	IV under potential control (E_s = 0.14 V vs SCE)	*IE* (bias = –0.1 V)
switching bias (V)	1.64 ± 0.30	0.8 ± 0.1	−0.69 ± 0.06
ratio of switching events to total events	0.8	0.47	0.21
peak position (V)	1.70 ± 0.15	0.8 ± 0.1	−0.75 ± 0.05

lower frequency of these peaks correlates with the disappearance of the R1/O1 peaks in the cyclic voltammetry. Indeed, these peaks are found to become less frequent on repeated cycling as the process R1/O1 diminishes in the CV. There is no feature in the CV at ca. 0.3 V vs SCE corresponding to peak 1. Few events have been recorded for it, so the evidence for this process is weaker. However, if there is indeed a redox process at this potential, then given that R1/O1 is barely visible in the cyclic volammograms it is not surprising that an even weaker feature cannot be seen.

(d) *IE* Measurements. Both NDR peaks and switching events were seen in *IE* curves taken at fixed bias. Switching events were rarer (21% of the total), and they occurred at essentially the same potential as the NDR peaks. Peaks in the *IE* curves are seen at ca. −0.75 V vs SCE while switching is observed at ca. −0.7V vs SCE when the bias is −0.1 V (last column of Table 1). This is close to the potential for the R2/O2 redox process at −0.67 V. Examples of NDR peaks are given in Figure 6a and 6b. Given the analysis of the *IV* curves under potential control just given, we would expect to see NDR peaks most frequently near the potential for the R2/O2 process but shifted by an amount equal to the applied bias. A statistical analysis of many curves is given for a bias of +0.1 V in Figure 6c and −0.1 V in Figure 6d. Applying a positive bias should enhance the local field, and indeed a peak is seen in the distribution near −0.57 V vs SCE for a bias of +0.1 V (Figure 6c). Conversely, the local field should be reduced by a negative bias, and a peak is seen in the distribution near −0.77 V vs SCE for a bias of −0.1 V (Figure 6d). These values are exactly what is expected for $\alpha = 1$.

IE data showed more variability than *IV* data, and the data analyzed above were selected from curves that showed a strong (and narrow) current peak. A significant subset of the *IE* curves showed peak values *that did not depend on tip bias* (examples are shown in the Supporting Information). These curves tended to have smaller peak values of current, suggesting that the tip was not strongly bonded to the molecule (which would lead to $\alpha = 0$). To test this hypothesis, we took data starting with the tip deliberately placed further from the monolayer surface. In this case almost none of the NDR curves showed a bias-induced shift, consistent with $\alpha = 0$ for the weaker coupling. Why is this subpopulation seen in *IE* curves but a corresponding subpopulation is not seen in *IV* curves? The answer to this question is straightforward: structure in the *IV* curve owing to bias-induced changes of oxidation states *requires* strong coupling of the tip to the molecule to overcome the electrochemical potential. Data taken with weak coupling would yield linear characteristics with much smaller currents and would probably be impossible to distinguish from the leakage background.

Another type of *IE* curve that sometimes occurred was much broader with higher peak currents (data not shown). Gaps showing such curves were much more stable, and we speculate that these arose from the trapping of multiple molecules across the gap. We note that in breakjunction measurements of the response of oligoanilines show very sharp NDR peaks when individual molecules are trapped in the gap, but the averaged data for many molecules give a much broader peak.[6]

(e) Control Experiments with BP. In the control *IE* experiments with BP, most curves are featureless. We only infrequently observed a nonreversible current peak (∼10% of total curves) or a switching event (∼10%) near −0.7 V when a low tip bias was used. Typical featureless curves are shown in Figure S4a and represent about 80% of the curves. Two examples of the 10% of *IE* curves with current peaks are shown in Figure S4b. The rare current peaks and current switching events may correlate with the reduction peak of BP around −0.71 V (Figure 2b).

Discussion

Experiments under potential control strongly suggest that the origin of the switching at a bias of ca. 1.6 V in dry samples and in an inert environment is likely related to changes of the oxidation state of the BPDN molecules. Electrochemical potential scales and work functions can be related, subject to a

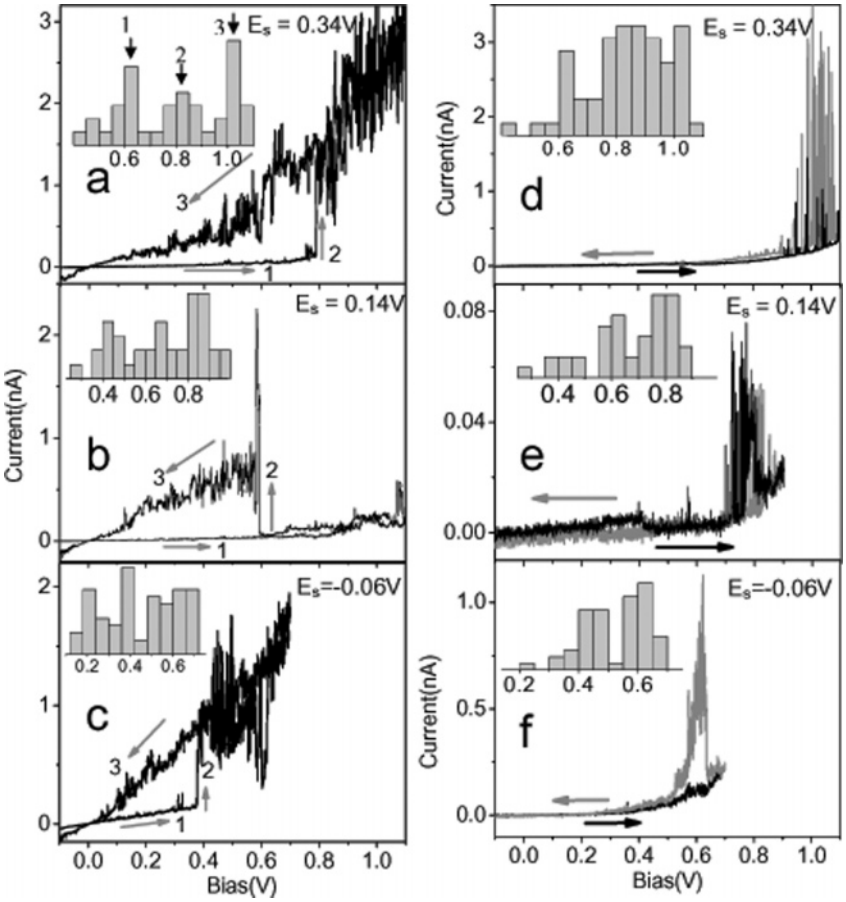

Figure 4. *IV* curves collected in 50 mM $Na_2B_4O_7$ aqueous electrolyte, shown as a function of potential vs SCE. The left column (a, b, and c) shows representative *IV* curves that exhibit current switching, and the right column (d, e and f) shows representative *IV* curves the exhibit current peaks (NDR) at (from top to bottom) 0.34 V, 0.14 V, and −0.06 V vs SCE. Note how the features (switching or NDR peaks) shift to lower bias as the substrate is made less positive. The inset at the upper left corner of each panel is the histogram of the bias for current switching (left column) or current peaks (right column) at a corresponding surface potential (bin size 50 mV). The starting current was 10−30 pA (at a bias of 0.1 V), and the sweep rate was 1 V/s. The arrows and numbers show the directions and sequence of the bias sweeps.

Table 2. Peak Bias for the Three Switching Events and NDR Peaks Identified in the Histograms Shown in Figure 4; α and $E_p(0)$ Are Calculated Using eq 3

		E_s (V vs SCE)				
		−0.06	0.14	0.34	α	$E_p(0)$
switching events	peak 1 (V)	0.23 ± 0.06	0.41 ± 0.06	0.57 ± 0.11	1.2 ± 0.04	−0.33 ± 0.02
	peak 2 (V)	0.41 ± 0.08	0.60 ± 0.09	0.80 ± 0.07	1 ± 0.02	−0.48 ± 0.01
	peak 3 (V)	0.59 ± 0.07	0.86 ± 0.09	0.98 ± 0.07	1 ± 0.2	−0.69 ± 0.2
NDR peaks	peak 1 (V)	0.23[a]	0.40 ± 0.06	0.64 ± 0.09	0.98 ± 0.1	−0.27 ± 0.04
	peak 2 (V)	0.43 ± 0.06	0.62 ± 0.08	0.83 ± 0.07	1 ± 0.03	−0.49 ± 0.02
	peak 3 (V)	0.57 ± 0.07	0.79 ± 0.08	0.95 ± 0.06	1 ± 0.1	−0.67 ± 0.08

[a] Insufficient data to calculate standard deviation

number of assumptions, as discussed elsewhere.[33] Using the 0.24 V difference between the SCE and NHE reference electrode, we can align the Fermi level of the gold electrode (ca. 5.3 V below vacuum) to the redox potential of BPDN molecule (−0.66 V, vs SCE, ca. 4 V below vacuum) as illustrated in Figure 7. Thus, 5.3 V − 4 V = 1.3 V of bias is needed to bring the Fermi level of the gold tip up to the molecule's formal potential, close (given the uncertainties in potential distribution in these conditions) to the observed value of 1.6 V.

Resonant tunneling[34] or enhanced hopping via sequential reduction−oxidation processes[35,36] may occur when the electrode Fermi level and molecular formal potentials align. Either case will lead to a sigmoidal *IV* and peak in *IE* if molecular states remain stable (though the two cases are distinguished by a small shift owing to the unknown reorganization energy[37]). However, bias-induced changes in the molecule can lead to peaks (and switching events) in *IV* curves. As listed in Table 1, 80% of the curves obtained in toluene show switching and 20% of the curves show an NDR peak. If reduction of the molecules is nonreversible, this could change the electronic levels ap-

(33) Han, W.; Durantini, E. N.; Moore, T. A.; Moore, A. L.; Gust, D.; Rez, P.; Leatherman, G.; Seely, G. R.; Tao, N.; Lindsay, S. M. *J. Phys. Chem.* **1997**, *101*, 10719−10725.

(34) Schmickler, W.; Widrig, C. *J. Electroanal. Chem.* **1992**, *336*, 213−221.

(35) Kuznetsov, A.; Somner-Larsen, P.; Ulstrup, J. *Surf. Sci.* **1992**, *275*, 52−64.

(36) Kuznetsov, A. M.; Ulstrup, J. *Electron transfer in chemistry and biology*; Wiley: New York, 1999.

(37) Schmickler, W.; Henderson, D. *J. Electroanal. Chem.* **1990**, *290*, 283−291.

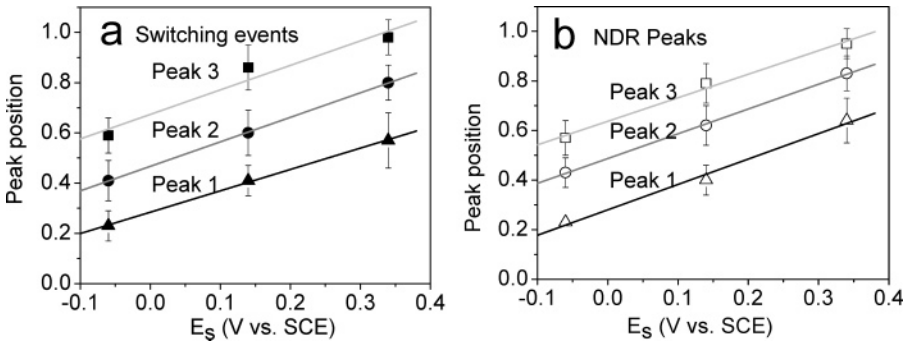

Figure 5. Plots of the peak value of the switching bias (a) or NDR peak bias (b) as a function of surface potential for the three peaks shown in the histograms in Figure 4. Solid lines are fits to eq 3 that yield the values of α and $E_p(0)$ listed in Table 2.

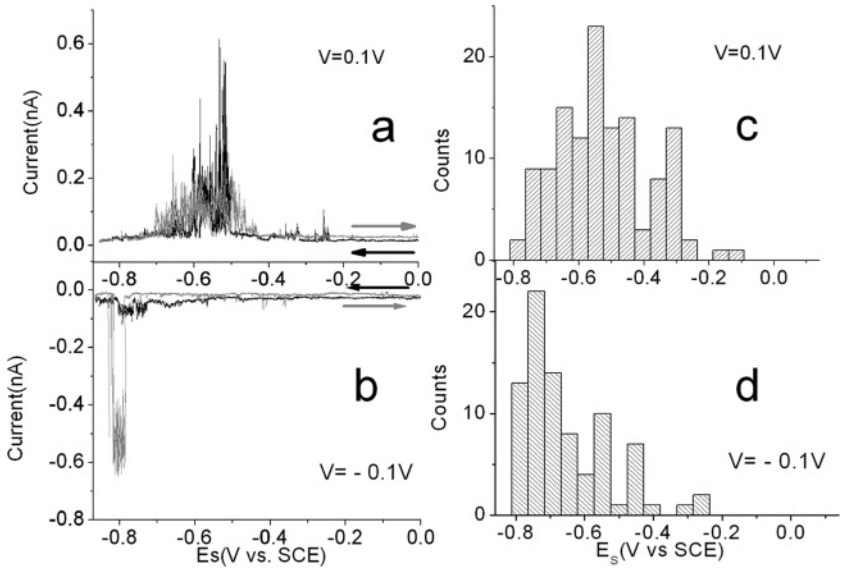

Figure 6. Typical *IE* curves taken in 50 mM $Na_2B_4O_7$ aqueous electrolyte for BPDN at fixed bias values of −0.1 V (a) and 0.1 V (b). The surface potential was scanned from 0 V to −0.87 V (black curves) and back to 0 V (gray curves). Histograms of potentials for conductance peaks (bin size = 48mV) are shown in (c) (bias = −0.1 V) and (d) (bias = 0.1 V).

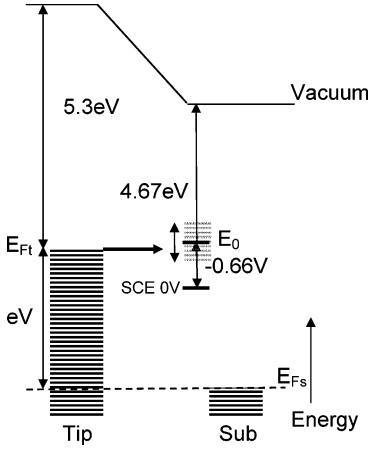

Figure 7. Proposed mechanism for the bias-induced switching near 1.6 V when the surface is not under potential control. E_0 is the redox potential of the molecule with uncertainty displayed as a band. E_{Ft} and E_{Fs} are Fermi levels of the gold tip and gold substrate, respectively. *V* is the applied bias.

preciably, causing switching or a peak. One might ask how such electrochemical behavior can be observed without counterions surrounding the molecule, but it is possible that the anion could be stabilized by an image charge in the electrodes[38,39] and/or conformational changes of the molecule.[40] Due to the distance between the redox center and the electrode (on the order of 1 nm) the image charge effect is presumably small.[41] Therefore the internal conformational changes may be the major factor stabilizing the anion when the molecule is not in an electrolyte. This is the explanation of switching offered by Derosa et al.:[40] the two pyridine rings can twist 82° to form a coplanar conformation to accommodate the extra electron trapped in the molecule. In their model, the consequent conformational changes of the molecule-induced level shifts lead to switching.

For *IV* curves taken in electrolyte under potential control, switching events and NDR peaks occur with equal probabilities at the redox potential of the molecule (E_t = −0.67 V). The increased appearance of NDR peaks may reflect more *reversible* reduction events of the molecule. If the anion is stabilized by the counterions surrounding the molecule, internal conformational change may be less likely because the anion is rapidly screened by counterions. NDR events in electrolyte were found to be generally reversible (i.e., the sweep up overlays the sweep

(38) Zhu, X.-Y. *J. Phys. Chem. B* **2004**, *108*, 8778−8793.
(39) Kubatkin, S.; Danilov, A.; Hjort, M.; Cornil, J.; Bredas, J.-L.; Stuhr-Hansen, N.; Hedegard, P.; Bjornholm, T. *Nature* **2003**, *425*, 698−701.
(40) Derosa, P. A.; Guda, S.; Seminario, J. M. *J. Am. Chem. Soc.* **2003**, *125*, 14240−14241.
(41) Vesper, B. J.; Salaita, K.; Zong, H.; Mirkin, C. A.; Barrett, A. G. M.; Hoffman, B. M. *J. Am. Chem. Soc.* **2004**, *126*, 16653−16658.

down). Switching events were not (by definition, the conductance remains changed until after a large change in bias or potential) so the switching probably occurs when the molecules undergo an irreversible change. It seems likely that such irreversible changes would occur more frequently when the molecule is not in a supporting electrolyte (i.e., in toluene or in air), and this would account for the higher frequency of switching events observed in these conditions. Note, however, that both switching events and NDR peaks are clearly associated with the reduction of the molecule. The reversibility of NDR events in *IV* curves is not as good as that of the current peaks in *IE* curves. This may reflect the higher bias used in *IV* measurements which could pin the conformation of the molecule in the gap.

In *IE* experiments (especially when the starting current is low or at small bias), we found a clear one-to-one correspondence between redox peaks in the CV and switching events (and/or current peaks) in *IE* curves. Table 2 shows how the potential for zero bias switching or NDR peaks coincided with the potentials for redox processes. However, we also noticed that switching events were relatively more frequent near the nonreversible redox process in the CV (ca. −0.47 V vs SCE). Similarly, the more reversible current peaks appeared more frequently near the reversible redox process in the CV (ca. −0.67 V vs SCE).

The reversible current peaks that occur in 80% of the events near the reversible redox potential of the BPDN molecule in *IE* measurements may be accounted for by resonant tunneling mediated through the available redox levels.[34−36] In this process (when the local potential reaches −0.67 V vs SCE), the redox level of the BPDN molecules is brought into the energy gap between the electrode Fermi levels owing to the surface potential (weak coupling case) or tip potential (strong coupling case). Solvent reorganization energy in this system is likely reduced owing to solvent confinement in the STM so that the peak current occurs when the molecular potential is close to the formal potential for the redox process.[20,42]

(42) Friis, E. P.; Kharkats, Y. I.; Kuznetsov, A. M.; Ulstrup, J. *J. Phys. Chem. A* **1998**, *102*, 7851−7859.

Conclusions

In summary, we performed in situ STM measurements of the current through a BPDN molecule with and without electrolyte (and potential control) both as a function of the surface potential at a fixed tip−substrate bias and as a function of the tip−substrate bias at fixed surface potential. The *IV* measurements in toluene and air agreed with previously published work on bias-induced switching. We found that switching occurred when the system was poised near a potential where redox processes occurred on the molecule. Switching (as opposed to the occurrence of a current peak) probably reflects nonreversible conformational changes in the molecule associated with the charging process. *IV* experiments in electrolyte under potential control showed both switching events and NDR peaks but at a lower bias. The switching bias and NDR peak bias-shifted with the surface potential, further demonstrating that the switching events and NDR peaks were related to the redox events on the molecule. Compared with the *IV* experiments, the *IE* experiments were performed at a much lower tip-to-substrate bias, with the result that fewer switching events were observed and more reversible current peaks were seen. The current peaks were attributed to resonant tunneling via reversible redox states. Taken together, the results of *IE* and *IV* experiments demonstrate clearly that the bias-induced switching of these molecules is a consequence of an electrochemically driven change in charge state of the molecule.

Acknowledgment. This work was supported by an NIRT grant of the NSF (to S.L.) and DARPA via the AFOSR (to J.M.T.).

Supporting Information Available: Complete details of synthesis and molecular characterization. Cyclic votammograms of BPDN in organic solvent, BPDN thiol reduction in aqueous solution. Switching associated with BPDN nonreversible redox peaks and current peaks associated with BPDN reversible redox peak. This material is available free of charge via the Internet at http://pubs.acs.org.

JA0635433